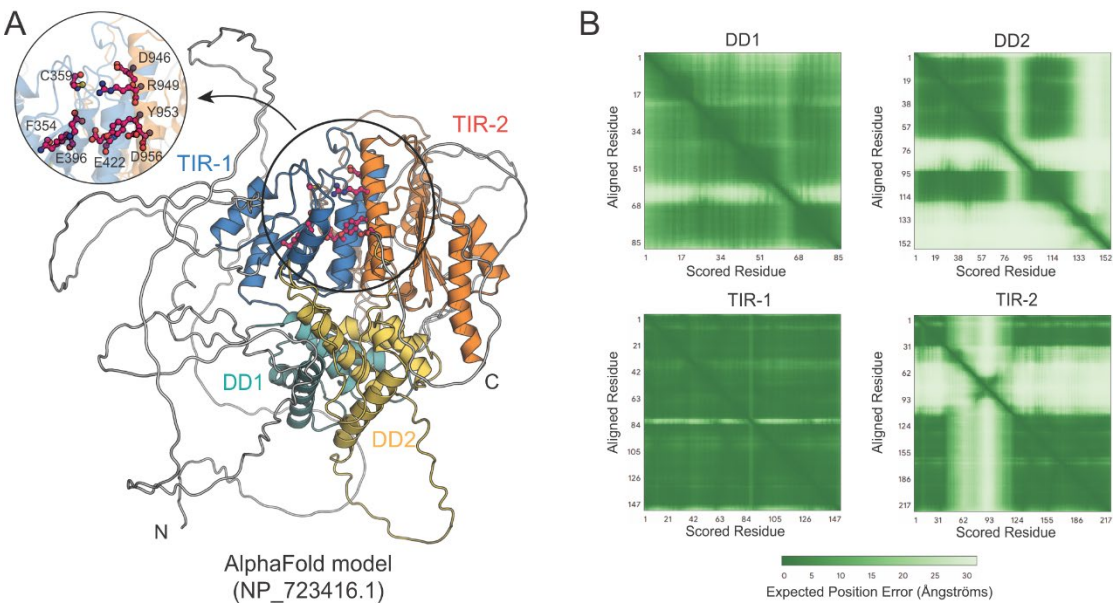

Supplementary Figure S1. Supplementary data related to Figure 1. (**A**) AlphaFold model of full-length Raw (NP_723416.1). The four structured domains are highlighted, with a predicted catalytic pocket formed by a cluster of highly conserved residues located within the TIR-1 and TIR-2 domains. (**B**) PAE (Predicted Aligned Error) plots for each of the four structured domains of Raw.

Supplementary Figure S2. Supplementary data related to Figure 1. Multiple sequence alignment (MSA) of Raw TIR-1 domain, TIR-2 domain, bacterial Raw-like TIR domain, and other known eukaryotic TIR domains. The Raw sequences in MSA are labelled by species abbreviation followed by their NCBI accession numbers, while other known eukaryotic TIR sequences are presented by their family name followed by the Protein Data Bank (PDB) IDs. The secondary structure is shown above the MSA, while the consensus is displayed below the MSA. The MSA was colored according to the consensus in 80% of the sequences based on 7 amino acid classes. Coloring theme: the amino acid involved in either catalytic activities or

specific function is highlighted in red background with white font color and bold font style; any amino acid present above the threshold is highlighted in black background with white font color and bold font style; hydrophobic (h) in yellow background with bold font style; aromatic groups (a) in orange background with bold font style; big amino acids (b) in light grey background with bold font style; small amino acids (s) in green background with bold font style; polar (p) group in blue background with bold font style; charged (c) amino acids in pink background with bold font style.

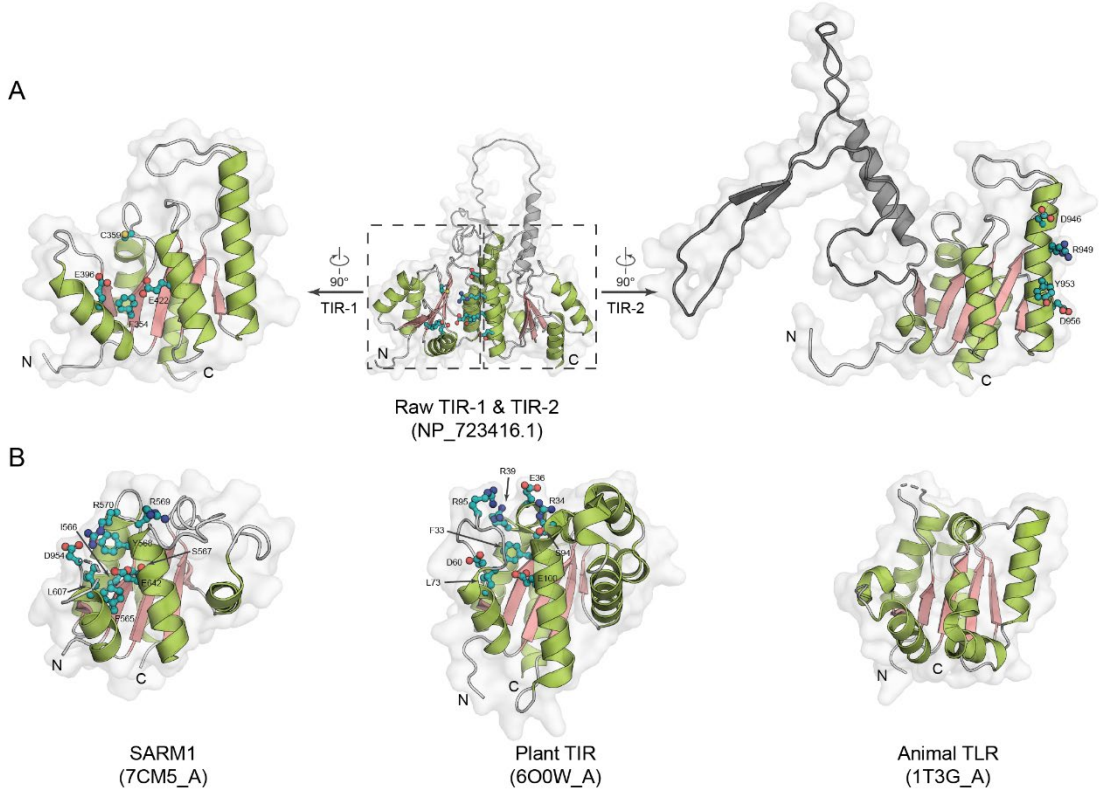

Supplementary Figure S3. Supplementary data related to Figure 1. Representative ribbon structures are shown for (**A**) the Raw TIR-1 and TIR-2 domains and (**B**) the SARM1-TIR domain (left), plant NLR-TIR domain (center), and animal TLR-TIR domain (right). In these models, α-helices are depicted in green and β-sheets in pink, while loops and other non-conserved regions are rendered in grey. Predicted catalytic residues for each family are illustrated using ball-and-stick representations, with carbon atoms in teal, nitrogen atoms in blue, oxygen atoms in red, and sulfur atoms in orange.

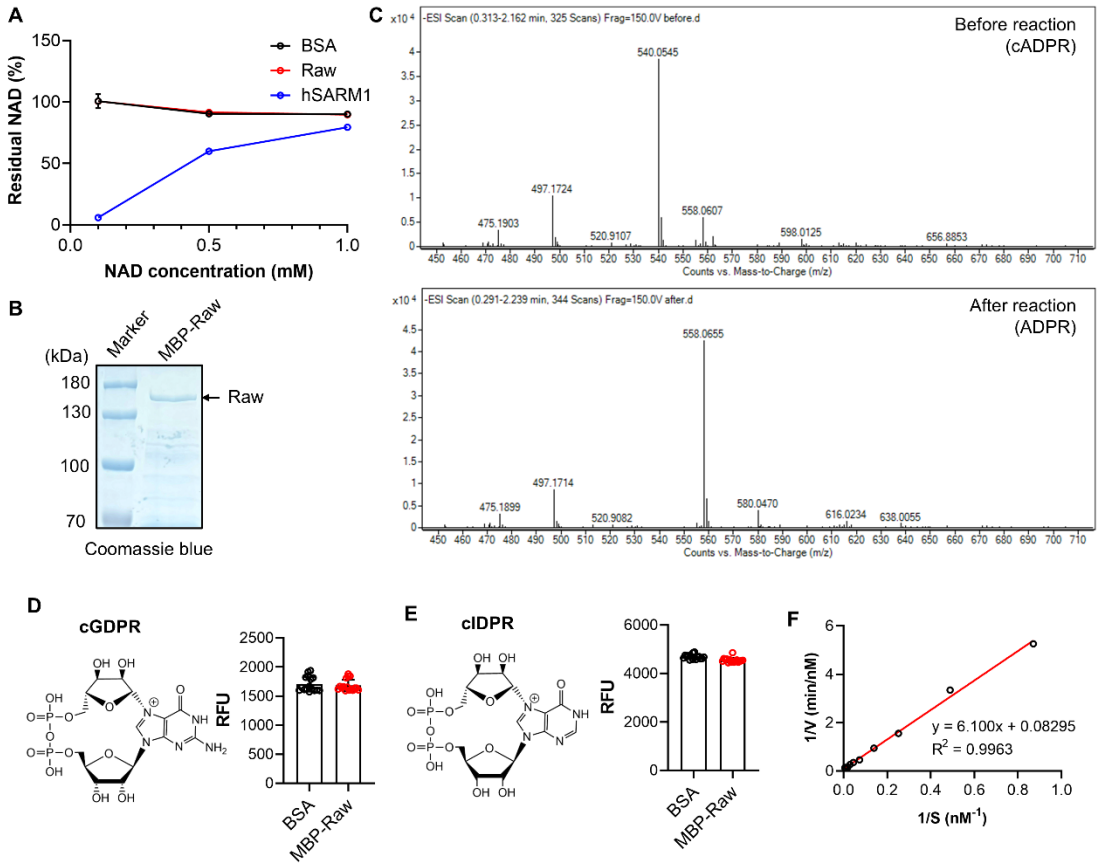

Supplementary Figure S4. Supplementary data related to Figure 2. (**A**) BSA, purified hSARM1 and Raw (final 5 µg/ml) were incubated with 0.1, 0.5 and 1.0 mM NAD for 4 h, with 0.1 mM NMN included in hSARM1's reaction. Residual NAD was measured using the cycling assay. (**B**) Purified recombinant MBP-Raw protein was analyzed by Coomassie Brilliant Blue staining to assess its purity and integrity. (**C**) LC–MS analysis of cADPR before (upper) and after (lower) reaction with purified MBP-Raw. MBP-Raw (5 µg/ml) was incubated with 0.1 mM cADPR for 4 h, and aliquots taken before and after reaction were analyzed on an Agilent 6540 Quadrupole-TOF LC/MS. (**D-E**) Structures of cGDPR (D) and cIDPR (E) are shown alongside the results of their incubation with purified MBP-Raw (5 µg/µl; 10 µM compounds). **Detailed methods:** To generate cGDPR and cIDPR, 25 µg of *Aplysia* ADP-ribosyl cyclase[1] was incubated overnight at room temperature with 100 µl of 50 µM NGD or NHD in KHM buffer (110 mM potassium acetate, 20 mM Hepes, pH 7.4, 2 mM $MgCl_2$). Cyclase was removed by filtration through a 0.22 µm PVDF membrane. The resulting cGDPR and cIDPR (10 µM) were then incubated with MBP-Raw or a control protein, BSA (5 µg/mL), for 6 hours at room temperature. Fluorescence measurements (excitation/emission: 300 nm/410 nm) were performed using an Infinite M200 PRO microplate reader (Tecan). (**F**) Lineweaver-Burk plot corresponding to Figure 2F.

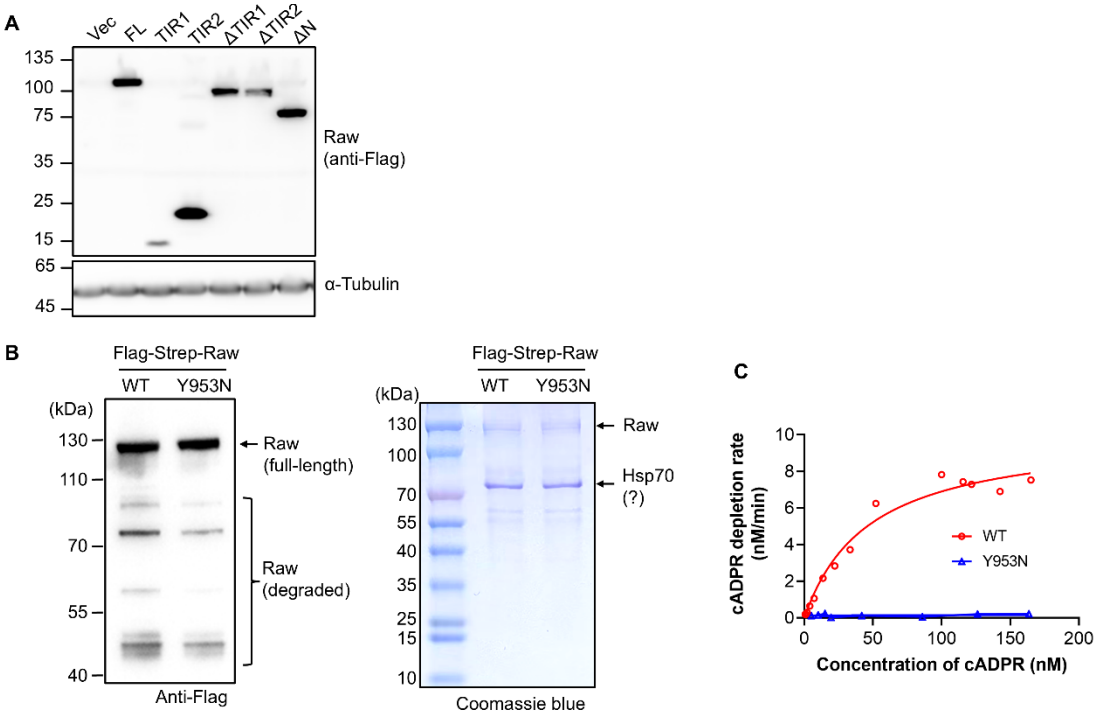

Supplementary Figure S5. Supplementary data related to Figure 3. (**A**) *Drosophila* S2 cells were transfected with vectors encoding various truncations of Raw. After 48 hours, cell lysates were subjected to Western blots. (**B**) Flag-Strep-tagged wildtype or Y953N mutant Raw was expressed in HEK-293F cells. Purified proteins were assessed by Western blot (left) and Coomassie Brilliant Blue staining (right). **(C)** Michaelis-Menten kinetic analysis of Raw-mediated cADPR depletion, as in Figure 2F, with the Y953N mutant included as a negative control.

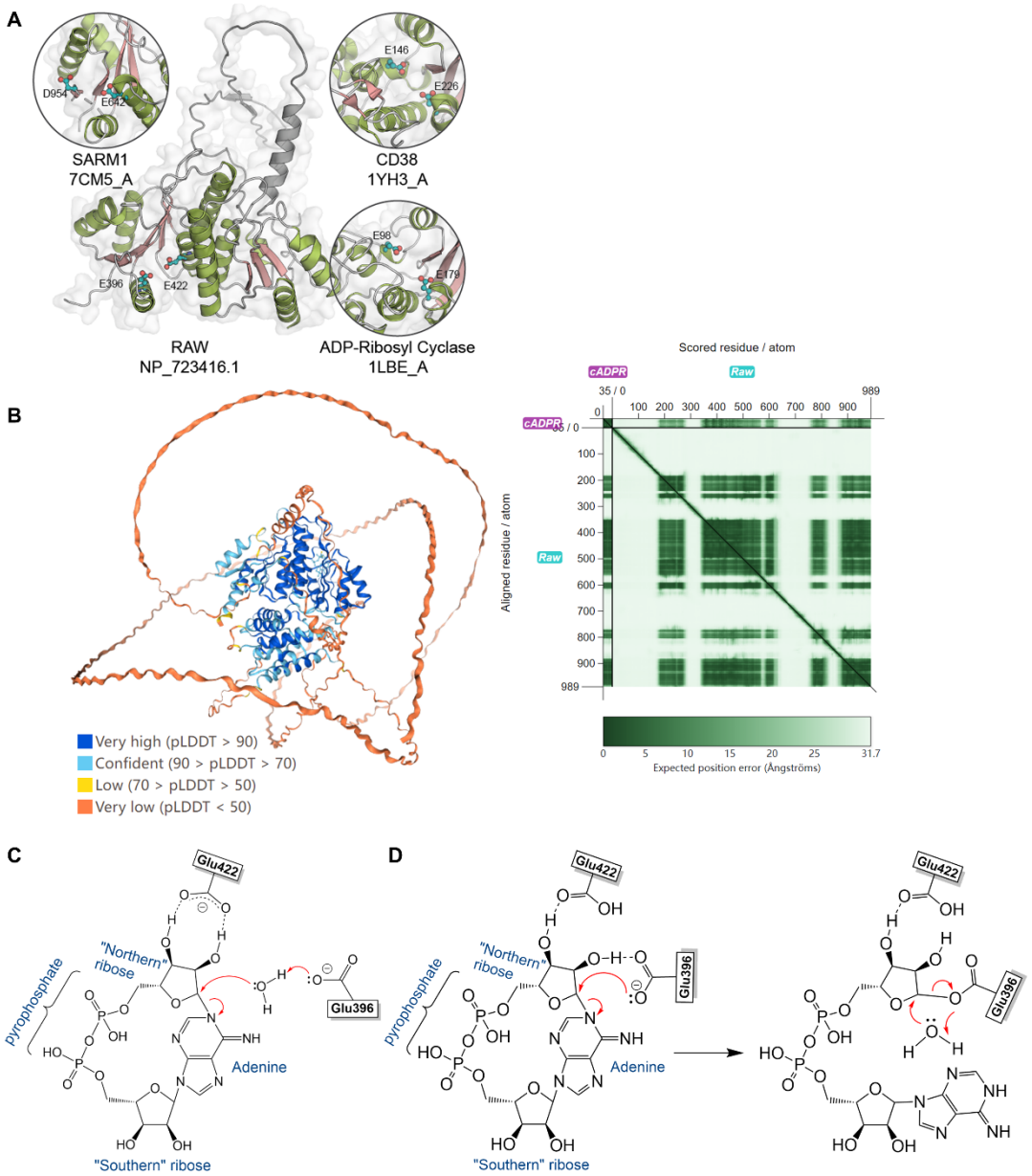

Supplementary Figure S6. Supplementary data related to Figure 3. (**A**) Predicted catalytic pocket of Raw and comparison with the one in SARM1, CD38, and ADP-ribosyl cycles. The α-helices and β-sheets of the structures are shown in green and pink, respectively, while the loop and other non-conserved regions are shown in grey. The predicted catalytic residues for each family are shown as balls and sticks, with carbon atoms in teal, nitrogen atoms in blue, oxygen atoms in red, and sulfur atoms in orange. (**B**) Structural prediction of the Raw/cADPR complex. (**C-D**) Proposed mechanisms of Raw-catalyzed cADPR hydrolysis.

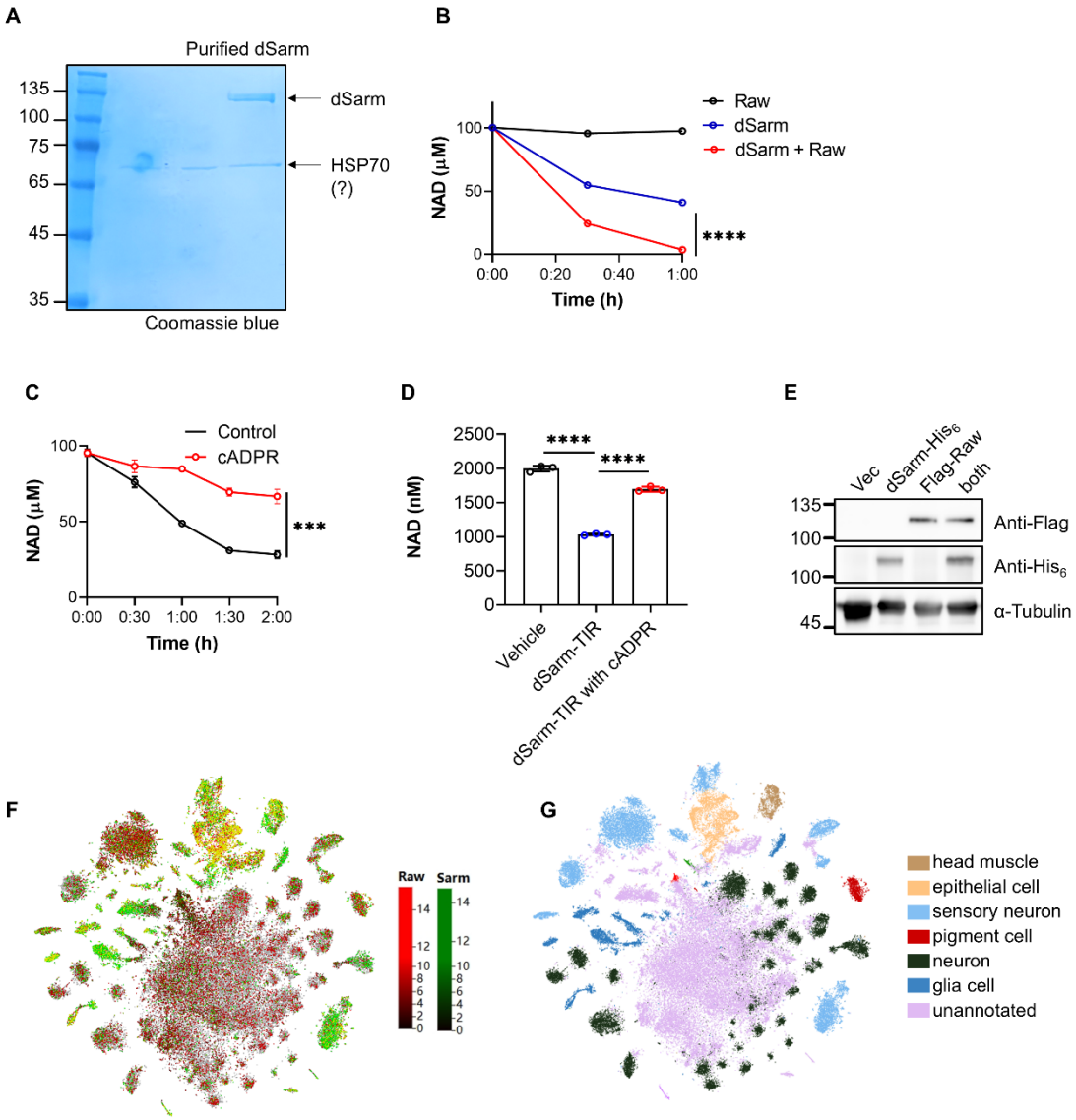

Supplementary Figure S7. Supplementary data of Figure 4. (**A**) Coomassie brilliant blue staining of recombinant protein Strep-tagged dSarm. Stably expressed dSarm cell line was generated using lentivirus. Protein was purified by Step-Tactin beads. (**B**) Time-course analysis of NAD depletion by dSarm and/or Raw (final 100 μg/mL) starting from 100 μM NAD. Remaining NAD was quantified every 30 min using the cycling assay. (**C**) Effect of cADPR on the NAD-consuming activity of dSarm. Recombinant dSarm (final 100 μg/mL) was incubated with 100 μM NAD, either alone or in the presence of 100 μM cADPR, for the indicated times. Remaining NAD was quantified using the cycling assay. (**D**) cADPR inhibits dSarm-TIR's enzymatic activity. 2 μM NAD was incubated with 10 μg/ml dSarm-TIR with or without 2 μM cADPR at room temperature for 2 h. The remaining NAD was measured using the cycling assay[2]. (**E**) Western blot analysis demonstrates the expression of His-tagged dSarm and/or Flag-tagged Raw in S2 cells. (**F-G**) tSNE plots of head cells from the FCA Stringent 10x dataset. e, expression levels of Raw and dSarm, with the expression data log-transformed and CPM (Counts Per Million) normalized. g,

detailed annotations of cell types or clusters. Data were obtained from Fly Cell Atlas[3] and visualizations were created using SCope[4] (https://flycellatlas.org/scope).
The experiment was repeated three times, and data are presented as means ± SDs (n = 3). Statistical significance was determined using one-way ANOVA test (****, $P < 0.0001$).

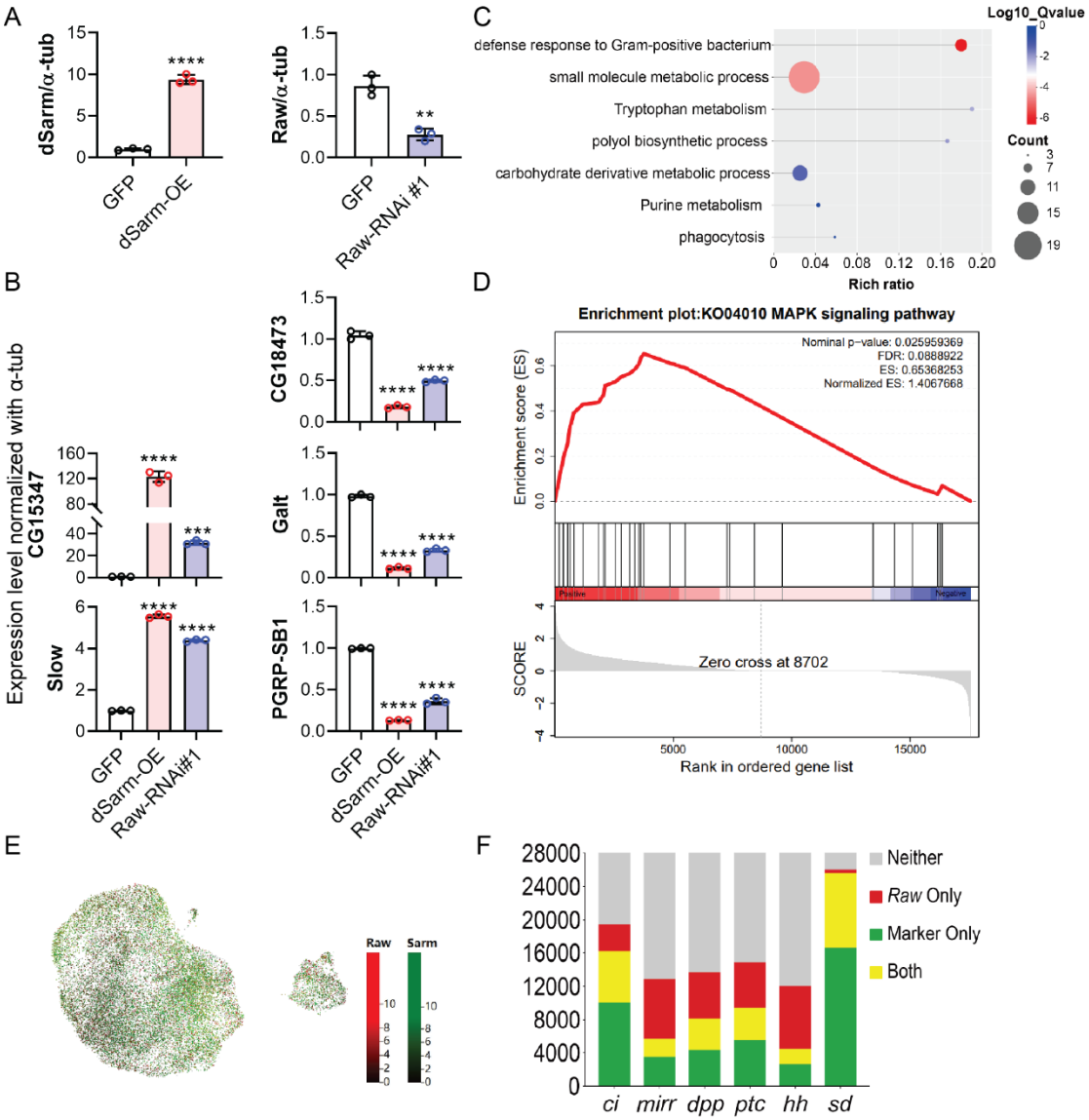

Supplementary Figure S8. Supplementary data of Figure 5-6. (**A**) S2 cells were transfected with the plasmids encoding the dSarm and the dsRNA of Raw. The expression levels of dSarm and Raw were quantified by qRT-PCR. (**B**) The expression levels of the downstream genes were measured by qRT-PCR in S2 cells overexpressing dSarm or knocking down Raw. (**C**) Downregulated DEG Enrichment Analysis results, illustrating significantly downregulated pathways following 8-Br-cADPR treatment. Enrichment analysis results were generated by Metascape (https://metascape.org/) with GO, KEGG, Reactome databases. The X-axis represents the enrichment ratio (Rich ratio = Term Candidate Gene Num/Term Gene Num). The bubble size represents the number of genes annotated to the pathway. The color represents the Q-value that accounts for the FDR. The red color indicated a lower FDR. (**D**) GSEA enrichment plot that 8-Br-cADPR-treated groups compared to control groups generated for the KEGG pathway "KO04010 MAPK signaling pathway". (**E**) tSNE plot (each dot represents a cell) demonstrating the expression of *dSarm* and *Raw* in wing imaginal disc. Data were obtained from the FCA public dataset (2F63d972e0_20200313__Ji_et_al_2019_Larvae_Wing_Disc.BBKNN).

dSarm-positive cells are marked in red, *Raw*-positive cells are marked in green, positive cells for both *dSarm* and *Raw* are marked in yellow, and cells negative for both are marked in grey. (**F**) The distribution of Raw and genes essential for wing development in the same wing disc cells in (E), including *Ci*, *mirr*, *dpp*, *ptc*, *hh*, and *sd*, in wing disc cells, showing their co-occurrence. All experiments in (A) and (B) were repeated at least three times, and data are presented as means ± SDs (n = 3). Statistical significance was determined using one-way ANOVA test (**, $P < 0.01$; ***, $P < 0.001$; ****, $P < 0.0001$).

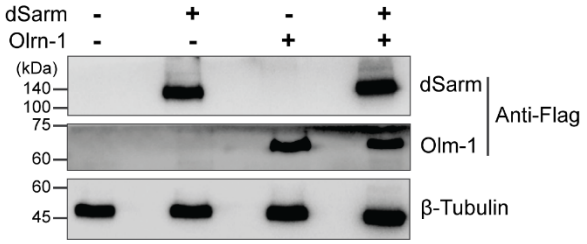

Supplementary Figure S9. Supplementary data of Figure 7. Western blot analysis demonstrates the over-expression of Flag-tagged dSarm and/or Olrn-1 in HEK-293T cells.

Supplementary Table S1: RNAseq datasets used for expression analyses.
Provided as a separate Excel file (Table S1.xlsx).

Supplementary Table S2: GO term enrichment and expression data of DEGs for each GO term.
Provided as a separate Excel file (Table S2.xlsx).

Supplementary Table S3: Primer sequences used in this study.
Provided as a separate Excel file (Table S3.xlsx).

Reference

1. Lee, H.C., and Aarhus, R. (1991). ADP-ribosyl cyclase: an enzyme that cyclizes NAD+ into a calcium-mobilizing metabolite. Cell Regul *2*, 203-209. 10.1091/mbc.2.3.203.
2. Graeff, R., and Lee, H.C. (2002). A novel cycling assay for cellular cADP-ribose with nanomolar sensitivity. Biochem J *361*, 379-384. 10.1042/bj3610379.
3. Li, H., Janssens, J., De Waegeneer, M., Kolluru, S.S., Davie, K., Gardeux, V., Saelens, W., David, F.P.A., Brbic, M., Spanier, K., et al. (2022). Fly Cell Atlas: A single-nucleus transcriptomic atlas of the adult fruit fly. Science *375*, eabk2432. 10.1126/science.abk2432.
4. Davie, K., Janssens, J., Koldere, D., De Waegeneer, M., Pech, U., Kreft, L., Aibar, S., Makhzami, S., Christiaens, V., Bravo Gonzalez-Blas, C., et al. (2018). A Single-Cell Transcriptome Atlas of the Aging Drosophila Brain. Cell *174*, 982-998 e920.

10.1016/j.cell.2018.05.057.